*Communication*

# Hydroxychloroquine Enhances Cytotoxic Properties of Extracellular Vesicles and Extracellular Vesicle-Mimetic Nanovesicles Loaded with Chemotherapeutics

**Sergey Brezgin [1,2], Anastasiya Kostyusheva [1], Natalia Ponomareva [1,2], Ekaterina Bayurova [3], Anastasia Frolova [2,4], Olga Slatinskaya [5], Landysh Fatkhutdinova [6], Georgy Maksimov [5], Mikhail Zyuzin [6], Ilya Gordeychuk [3], Sergey Makarov [6,7,8], Alexander Ivanov [9], Andrey Zamyatnin [2,4], Vladimir Chulanov [1,2,10], Alessandro Parodi [2,*], and Dmitry Kostyushev [1,2]**

[1] Laboratory of Genetic Technologies, Martsinovsky Institute of Medical Parasitology, Tropical and Vec-tor-Borne Diseases, First Moscow State Medical University (Sechenov University), Moscow 119991, Russia; Seegez@mail.ru, ponomareva.n.i13@yandex.ru, kostyusheva_ap@mail.ru, vladimir@chulanov.ru, dkostushev@gmail.com

[2] Division of Biotechnology, Sirius University of Science and Technology, Sochi 354340, Russia; Seegez@mail.ru, ponomareva.n.i13@yandex.ru, frolanasta@gmail.com, zamyatnin.aa@talantiuspeh.ru, vladimir@chulanov.ru, aparodi.sechenovuniversity@gmail.com, dkostushev@gmail.com

3 Chumakov Federal Scientific Center for Research and Development of Immunobiological Products, Russian Academy of Sciences (Polio Institute), 108819 Moscow, Russia; 79153645941@ya.ru, gordeychuk_iv@chumakovs.su

4 Institute of Molecular Medicine, First Moscow State Medical University (Sechenov University), Moscow 119991, Russia; frolanasta@gmail.com

5 Lomonosov Moscow State University, Faculty of Biology, Moscow, Russia 119991; slatolya@mail.ru, gmaksimov@mail.ru

6 School of Physics, ITMO University, Lomonosova 9, St. Petersburg, 191002 Russian Federation; l.fatkhutdinova@metalab.ifmo.ru, mikhail.zyuzin@metalab.ifmo.ru, s.makarov@metalab.ifmo.ru

7 Harbin Engineering University, Harbin 150001, China; s.makarov@metalab.ifmo.ru

8 Qingdao Innovation and Development Center, Harbin Engineering University, Qingdao 266000, China; s.makarov@metalab.ifmo.ru

9 Engelhardt Institute of Molecular Biology, Russian Academy of Sciences, Moscow, Russia 119991; aivanov@yandex.ru

10 Department of Infectious Diseases, First Moscow State Medical University (Sechenov University), Moscow 119991, Russia; vladimir@chulanov.ru

* Correspondence: aparodi.sechenovuniversity@gmail.com; Tel.: +7 (965) 439-90-09

**Abstract:** Because of their high biocompatibility, stability, ability to negotiate biological barrier passage, and functionalization properties, biological nanoparticles have been actively investigated for many medical applications. Biological nanoparticles, including natural extracellular vesicles (EVs) and synthetic extracellular vesicle-mimetic nanovesicles (EMNVs) represent novel drug delivery vehicles that can accommodate different payloads. In this study, we investigated EVs and EMNVs for their physical, biological and delivery properties and we showed that EMNVs have similar delivery properties compared to EVs. In addition, these nanotherapeutics were analyzed for their cytostatic properties in combination with the FDA-approved drug hydroxychloroquine (HCQ), which increased their cytostatic thanks to its lysosome-destabilizing properties. Altogether, these data demonstrated that, at least in vitro, the use of synthetic biomimetic particles is comparable to the natural counterparts, while their synthesis is significantly faster and more cost effective. In addition, we highlighted the benefits of combining biological nanoparticles with a lysosome destabilizing agent that increased the delivery properties of the particles.

**Keywords:** exosomes; extrusion; proteolipid nanoparticles; drug delivery; nanomedicine; doxorubicin; extruded nanoparticles; hydroxychloroquine; endolysosomal escape; lysosomotropic

 doi:10.20944/preprints202212.0060.v1

## 1. Introduction

Bio-inspired and biological nanoparticles are currently under significant investigation for their potentialities in drug delivery [1]. Within the large portfolio of biological carriers [2], extracellular vesicles (EVs) are one of the most investigated platforms in the field [3] and they were tested recently in clinical trials for anticancer treatment [4]. EVs are proteolipid nanoparticles derived from the endosomal compartment and secreted by the cell after the fusion with multivesicular bodies. These vesicles can provide the same biological identity as the cell source, including targeting properties [5]. EVs can be produced by any cellular phenotype [6]–[8] and can be loaded with different payloads, including small molecules [1] and biologics [9]. On the other hand, extracellular vesicle-mimetic nanovesicles (EMNV) are biological nanoparticles generated via active extrusion of cells through a series of filters with pores of decreasing diameter [10]. These nanoparticles comprise cell membrane enclosing the cytosol. Similar to EVs, EMNV may be derived from virtually any cell type [10]. However, EMNVs manufacturing does not require long-term culturing and processing of large amounts of cell culture media as compared to EVs. Their harvest is independent from the cell state and their synthetic yield (particle/cell ratio) remarkably exceeds that of EVs [11].

EVs have been investigated as drug delivery vehicles since 1960s and are considered the gold-standard of this kind of technology and immunologically safer [12]. The major drawbacks of EVs reside in the expensive and lengthy procedures of production and in the complexity of the post-synthetic manipulation to accommodate the payload, while preserving their structure [13]. On the other hand, EMNVs are more compatible with upscaling procedures of the final product [14] and characterized by a faster and cost-effective synthesis, while their manipulation and loading options (including pre-synthesis genetic engineering modifications on the source cells) are comparable to EVs [10]. Still, the practical use of EMNVs should be considered with caution because of potential contamination with unwanted cellular materials (i.e., nucleic acids) that can eventually affect their immunological tolerance [15]. In consideration of the inherent differences at the basis of the EV and EMNV synthesis, it is reasonable to expect that their therapeutic properties can change both in terms of loading yield and cytostatic properties.

The use of biological nanoparticles in practice is of particular relevance due to their highest biocompatibility, safety, stability, ability to cross biological barriers and potentialities to program the cargo loading and/or targeted delivery of the system [16]. Poor escape from endolysosomal compartment after nanoparticle internalization by recipient cells is one of the major problem in the field [17]. Overcoming the endolysosomal barrier is crucial for the effective use of nanomedicines, including EVs and, possibly, EMNVs. Potential strategies include the use of hydroxychloroquine (HCQ), an FDA-approved antimalarial drug, used for over 60 years in the clinic [18]. HCQ is a lysosomotropic agent that inhibits lysosomal acidification and activity of P-gp, increasing their osmotic pressure [19]. At the systemic level, HCQ improves nanoparticle delivery by reducing macrophage clearance of NPs [20] and normalizing tumor vasculature [21]. As a promising endosomal escape candidate, HCQ was conjugated with several synthetic nanotherapeutics and demonstrated increased cytotoxicity [22], [23].

In this work, for the first time, we (1) characterized the use of EMNVs for delivering chemotherapeutics in direct comparison with EVs biopharmaceutics and (2) investigated the potential use of HCQ for increasing the cytotoxic activity of these biological nanoparticles. In this effort, we used HEK293T cells as an experimental model since they were extensively used in the field for determining nanoparticles toxicity [24], and we loaded EVs and EMNVs with doxorubicin (DOX), representing one of the most tested payloads in the field [25].

We discovered that DOX-loaded EMNVs have similar cytotoxicity as EVs, that eventually resulted the most effective formulations. EMNVs demonstrated significantly higher cytotoxicity compared to free DOX. The use of HCQ destabilized lysosomes, facilitating

 doi:10.20944/preprints202212.0060.v1

endolysosomal escape of biologics, and dramatically enhanced cytotoxic activity of both EVs and EMNVs.

## 2. Materials and Methods

*Cell culture*

HEK293T cells were cultured in DMEM (PanEco, Moscow, Russia) supplemented with 10% Fetal bovine serum (FBS) (Cytiva, Logan, UT, USA), 2 mM L-glutamine, 100 U/mL penicillin and 100 µg/mL streptomycin (Gibco, UK). Cells were cultured at 37°C at the incubator with 5% CO2. For doxorubicin internalization experiments and experiments with caspase reporter system, HEK293T cell were seeded into 12-well plates at ~60% confluency. Caspase 3 activation was analyzed in HEK293T cells transfected with ZipGFP-Casp3 plasmid (ZipGFP-Casp3 was a gift from Xiaokun Shu, Addgene #81241)[26]. Transfection was performed as follows: plasmid DNA was added to NaCl solution (solution A). Solution B containing polyethylenimine in NaCl was prepared in parallel, incubated for 10 min, and gently mixed with solution A. Two solutions were incubated at RT for 10 min and then added to cells. The day after transfection, cell culture medium was discarded, and the cells were gently washed twice in PBS and fresh complete medium was added. For cell viability analysis, cells were seeded into 96-well plates with 30% confluency.

*Isolation of EVs*

For isolating EVs, HEK293T cells were conditioned in DMEM media supplemented with 10% EV-free FBS. FBS was depleted from EVs by ultrafiltration using Amicon Ultra-15 100 kDa filter devices (Merck Millipore, Darmstadt, Germany) as described previously [27]. Isolation of EVs from conditioned media was performed according to the protocol described by Heath et al. with modifications [28]. Conditioned media was consequently centrifuged at 300 × g (10 minutes), 2000 × g (10 minutes) and 10000 × g (10 minutes). Clarified media was applied onto the column filled with Macro-Prep DEAE Resin (Bio-Rad, USA), washed with 20 column volumes (CV) of buffer containing 50 mM HEPES and 100 mM NaCl, 10 CV of buffer containing 50 mM HEPES and 335 mM NaCl followed by elution with 50 mM HEPES/890 mM NaCl buffer. Eluate was concentrated with Amicon Ultra-15 (100 kDa) filter devices (Merck Millipore, Darmstadt, Germany) followed by 3 washes with PBS and re-concentration. Aliquots of isolated vesicles were lysed with RIPA buffer and diluted with PBS, and total protein amount in sample was measured with Pierce™ Coomassie (Bradford) protein Assay Kit (Thermo Fisher Scientific, Waltham, MA, USA).

*Preparation of EMNVs*

HEK293T cells (~$5\times10^6$) were washed twice with PBS and detached using Versene solution (PanEco, Moscow, Russia). Cell suspension was serially extruded 7 times through 10-, 5- and 1-µm polycarbonate membrane filters (Nuclepore, Whatman, Inc., Clifon, NJ) using mini-extruder (Avanti Polar Lipids, Birmingham, AL). Resulted solution was centrifuged at for 10 minutes at 2000 × g and the for 10 minutes at 10000 × g to discard cell debris; the supernatant was then filtered via Centrisart 1 (300 kDa) Concentrator (Sartorius®, Goettingen, Germany) followed by 3 washes with PBS and re-concentration step. Aliquots of isolated vesicles were lysed with RIPA buffer and diluted with PBS, and total protein amount in sample was measured with Pierce™ Coomassie (Bradford) protein Assay Kit (Thermo Fisher Scientific, Waltham, MA, USA).

*Transmission electron microscopy (TEM)*

TEM assay of EVs/EMNVs samples was performed as described previously [26]. Before measurements, 5 µL of the EVs/EMNVs samples were pipetted onto a 400-mesh copper grid with carbon-coated formvar film and incubated for 1 min. The excess solution was soaked off by blotting with a filter paper. Then the grid was rinsed by adding distilled water for 10 sec. The grid was placed on 10 µL of 2% uranyl acetate, followed by blotting

Preprints (www.preprints.org) | NOT PEER-REVIEWED | Posted: 5 December 2022 doi:10.20944/preprints202212.0060.v1

to remove excess liquid. This step was repeated twice. TE microscope LIBRA 200 FE HR, Carl Zeiss, was used to visualized EVs/EMNVs.

*Dynamic light scattering*

A Malvern Zetasizer NanoZS instrument (Malvern, Worcestershire, UK) was used for dynamic light scattering analysis of produced EVs and EMNVs. Each EV/EMNV preparation, diluted 1/1,000 in PBS filtered through 20 μM filter (Corning), was analyzed 5 times; 1,5 mL of diluted preparations were loaded into polystyrene cuvette (DTS0012, Malvern, UK). Analyses were performed at +25 °C (100 of measurements) using 20-mW helium/neon laser (633 nm). Data were analyzed in Zetasizer software 8.01.4906 (Malvern, UK). Z-potentials were analyzed in U-type cuvette (DTS1070, Malvern, UK) with gold electrodes. Measurements of ζ-potentials were performed at +25 ℃ at least 5 times. Background signal was measured in filtered PBS.

*Doxorubicin packaging*

EVs and EMNVs (1 mg of total protein) were loaded with doxorubicin by incubation with 400 μg/mL doxorubicin at 37° for 2 hours with shaking at 500 × rpm. Free doxorubicin was discarded by ultrafiltration using via Centrisart 1 (300 kDa) Concentrator (Sartorius®, Goettingen, Germany) followed by 3 washes with PBS. To estimate doxorubicin packaging efficiency, optical densities in samples were measured at 480 nm using spectrophotometer, and the amount of loaded doxorubicin was determined using calibration curve. Encapsulation efficiency was calculated as by the following formula: (doxorubicin amount incapsulated in vesicles)/(initial amount of doxorubicin for packaging) ×100%.

*Western blotting*

EVs/EMNVs preparations or HEK294T cells were lysed using 50 μl of RIPA buffer (50 mM Tris-HCl, pH 8.0, 150 mM NaCl 1% Nonidet P-40 (NP-40), 0.5% sodium deoxycholate, 0.1% sodium dodecyl sulphate (SDS), 1 mM sodium orthovanadate, 1 mM NaF) and incubated with agitation for 30 min at 4°C. Sample were then sonicated 30 sec and incubated on ice before analysis. Next, samples were loaded with 6× Laemmli buffer (5:1, 60 μg/well) onto 10% SDS-PAAG and then transferred on nitrocellulose membrane. Membrane was blocked with 5% milk in TBS-T (20 mM Tris, pH 7.5, 150 mM NaCl, 0.1% Tween 20) and stained with primary antibodies to exosome markers (EXOAB-KIT-1 for CD63, CD9, CD81 and Hsp70, SBI, USA) 1:1000 or to β-actin (A1978, Sigma, USA) 1:5000 in 5% milk in TBS-T overnight at 4°C. Membrane was washed trice with TBS-T and incubated for 1 hour with goat-anti rabbit-HRP conjugated antibodies (Ab6721, Abcam, USA) or with goat-anti mouse-HRP conjugated antibodies (Ab6787, Abcam, USA) diluted 1:5000 in 5% milk in TBS-T. Membrane was washed trice with TBS-T and chemiluminescent signal was developed with SuperSignal™ West Femto Maximum (Thermo Fisher Scientific, USA) and detected with X-ray film with 2 hours exposure.

*Flow cytometry analysis*

At harvest, cells were analyzed on a BD FACSCanto II flow cytometer (BD Biosciences, San Jose, CA, USA). Briefly, cell culture medium was discarded, and cells were washed twice in PBS, detached from the plates in trypsin-EDTA, resuspended in complete medium, and washed twice in PBS. EGFP-positive cells were detected in the FITC channel. Data were acquired with BD FACSDiva software and analyzed with NovoExpress software (ACEA Biosciences, San Diego, CA, USA).

*Cytotoxicity analysis*

HEK293T cells were seeded on 96-well plates at confluency ~30%. Cells were treated with (1) doxorubicin (1 μM), hydroxychloroquine (HCQ) (50 μM), or EV- or EMNV-loaded doxorubicin (500 nM) alone or in combination with 50 μM of HCQ for 12 hours. Afterwards, Cell Cytotoxicity Assay Kit Reagent (ab112118; Abcam, Cambridge, UK) was

Preprints (www.preprints.org) | NOT PEER-REVIEWED | Posted: 5 December 2022 doi:10.20944/preprints202212.0060.v1

added to cells according to manufacturer instructions. Optical density was measured using CLARIOstar Plus Microplate Reader in dynamics (2, 4, 21, 24 hours) to calculate relative viability of cells.

*Activated caspase 3 assay assay*

HEK293T cells were transfected with plasmid encoding ZipGFP-Casp3. ZipGFP-Casp3 was a gift from Xiaokun Shu Addgene 81241 [26]. ZipGFP-Casp3 encodes ZipGFP-based TEV protease reporter for apoptosis visualization. The reporter fluorescence was measured by FACS analysis.

*Lysotracker Assay*

HEK293T cells were incubated with 50 μM HCQ or 1 μM of Siramesine in complete FluoroBrite™ DMEM media for 24 hours. Next, LysoTracker™ Deep Red was added for 1 hour and visualized by fluorescent microscopy.

*Statistical analysis*

Values were expressed as the mean ± standard deviation (SD) in GraphPad Prism 7.0 software. Student's t-test or OneWay ANOVA, where applicable, with Tukey's HSD post hoc test were used to compare variables and calculate p values to determine statistically significant differences in means.

## 3. Results and discussion

### *3.1. Vesicle physical and biological properties*

First, we characterized the vesicle physical and biological properties (Figure 1) after EVs and EMNVs collection and generation from HEK293T cells, respectively, as reported in materials and methods section. TEM analysis showed that EVs and EMNVs are empty particles clearly defined by a proteolipid membrane (**Figure 1a,b**). EMNV shape resulted regular, while EV showed a certain aggregation level and deviation from spherical shape (**Figure 1a insets**). This phenomenon was already highlighted for EVs previously [29], while extrusion is likely the reason for the higher regular shape of EMNVs. DLS (Figure 1c) demonstrated that vesicles have a size between 120 and 140 nm with EMNVs larger than EVs (**Figure 1a,b,c,e**). Also, the vesicles resulted negatively charged (**Figure 1d**) and EMNVs showed a marked negative surface charge compared to EVs (-22 mV vs -15 mV). Due to the presence of proteins, a negative charge was expected in both the proteolipid vesicles and the lower EMNVs charge can be explained by a higher concentration of proteins on the surface of the system, different density of proteins in nanovesicles or, potentially, re-distribution of the surface charge upon aggregation [30], [31]. Size distribution analysis (**Figure 1e**) corroborated TEM analysis, showing a similar polydispersion index for both types of nanoparticles. The biological properties were defined by investigating 4 biomarkers currently representing the "dogma" [32] of biological particle characterization, including CD81, CD9, Hsp70, and CD63 (Fig 1f). All these biomarkers were positive and similar in band intensity in both the vesicles, tested in the same amount. More importantly, in comparison with the whole lysate of the cell source of the vesicles (HEK-293T), β-actin expression resulted insignificant and no specific bands were detected during the evaluation of the other markers. These data demonstrated that our synthetic route to produce EMNVs support the generation of a high pure product, very similar to EVs.

Preprints (www.preprints.org) | NOT PEER-REVIEWED | Posted: 5 December 2022 doi:10.20944/preprints202212.0060.v1

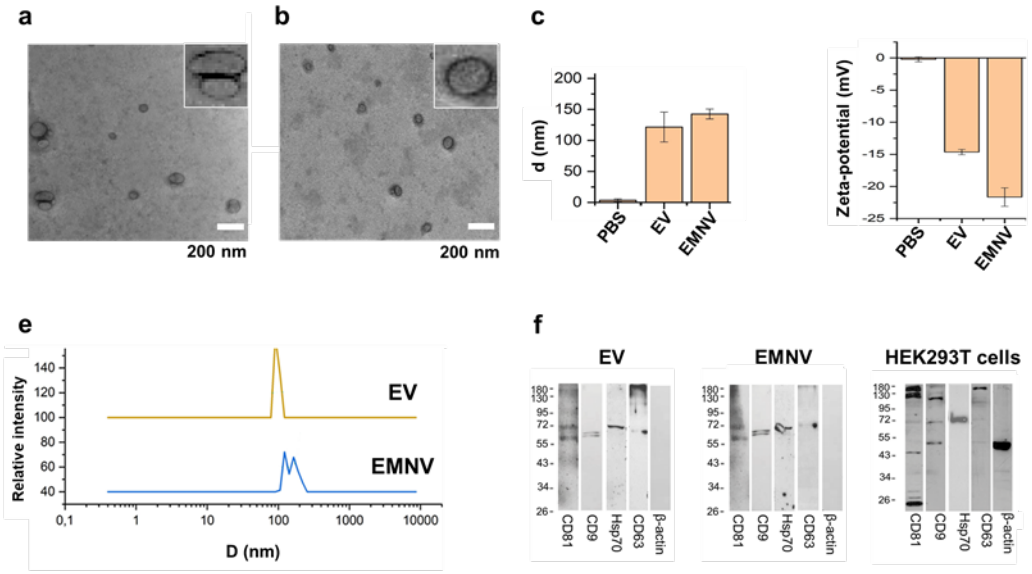


**Figure 1. Characterization of EVs and EMNVs.** TEM images of (a) EVs and (b) EMNVs with an enlarge image in an inset. The scalebar is 200 nm. DLS analysis of EVs/EMNVs (c) mean diameter, (d) zeta-potential and (e) polydispersity. (f) Western blot analysis of protein expression CD81, CD9, Hsp70, CD63 and β-actin in preparations of EVs, EMNVs and HEK293T cell lysates.

*3.2. Vesicle cytotoxic properties*

The yield of EMNVs was 60-fold higher than EVs secreted from the same amount of HEK293T cells (**Figure 2a**). Vesicle loading with doxorubicin was performed via passive method and loading yield was similar in both the particles, with EVs showing a slightly higher value of drug accommodation (**Figure 2b**). To directly compare the two types of nanoparticles (NPs) in their ability to deliver DOX, HEK293T cells were treated with free chemotherapeutic or DOX-loaded NPs. In addition, we introduced also an additional variable represented by a co-treatment with HCQ, to gather more insight about particle endosomal escape. As confirmed by **Figure 2c** depicting lysotracker red accumulation before and after HCQ treatment, this molecule decreased the probe fluorescent intensity in line with other papers showing its destabilizing activity on the cellular endosomal compartment and ability in favoring the intracellular drug release into the cytoplasm [33]. Particle internalization was evaluated via flow cytometry and both percentage of fluorescent cells and mean fluorescence intensity measures were analyzed (**Figure 2d, e**). Negative controls were represented by cells treated with empty NPs (mock) and HCQ alone to verify that these treatments did not increase cell fluorescence in the investigated channel. Six hours after treating cells with DOX-loaded NPs, the cells were viable and were detached to analyze NPs internalization (alone or in combination with HCQ).

Compared to untreated cells and negative controls (mock and HCQ), all the treatments with DOX-loaded EVs and EMNVs showed a similar percentage of positive cells higher than 90% (**Figure 2d**). However, analyzing the mean fluorescence intensity, the same samples showed a different internalization profile. Compared to cells treated with free DOX and DOX-loaded particles in combination with HCQ, the treatments performed with DOX-loaded EVs and EMNVs alone showed a significant reduction in fluorescence intensity (**Figure 2e**). This can be explained by the auto-quenching effect of the DOX, resulting higher when the vesicles are sequestered in the endosomal vesicles than in the cytoplasm [34].

Preprints (www.preprints.org) | NOT PEER-REVIEWED | Posted: 5 December 2022 doi:10.20944/preprints202212.0060.v1

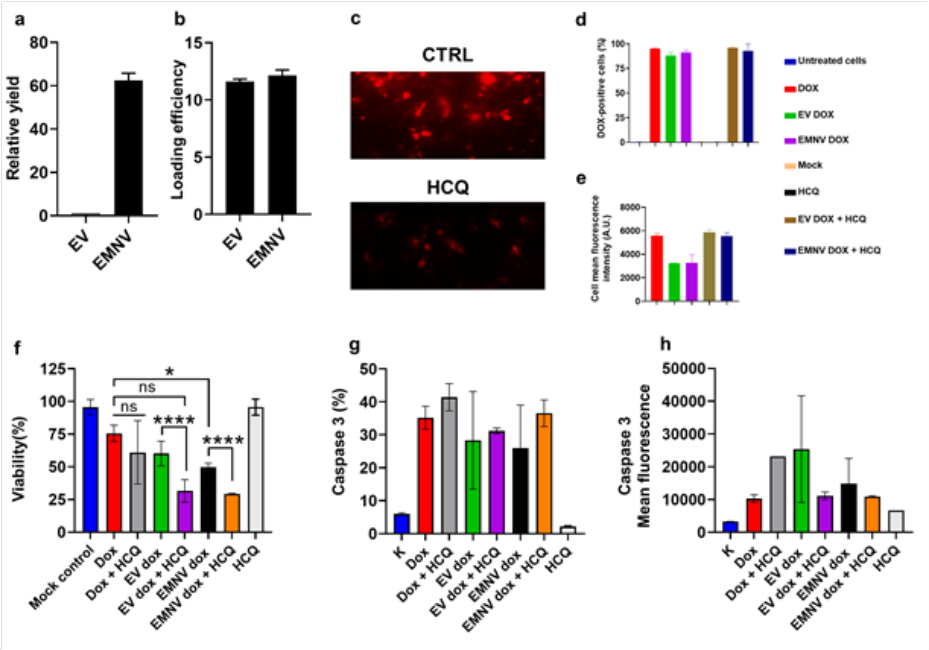


**Figure 2. Therapeutic properties of EVs and EMNVs and the effects of HCQ treatment.** (a) Relative yield of EVs and EMNVs. (b) Efficiency of DOX loading into EVs and EMNVs. (c) LysoTracker analysis of lysosome destabilization by HCQ (reduction of the LysoTracker signal in HCQ group). Internalization of free and EVs/EMNVs-encapsulated DOX and the effect of HCQ on DOX internalization measured by (d) percentage of DOX-positive cells and (e) mean fluorescence intensity. (f) Analysis of HEK293T cell viability with different treatments 24 hours post treatment. (g) Percentage of activated caspase 3-positive cells. (h) Mean fluorescence of activated caspase 3. *p<0.05; **p<0.01; ***p<0.001; ****p<0.0001.

These data were corroborated by the analysis of cell viability performed after 24 hours of treatment, demonstrating that, despite HCQ alone did not have any toxic effect nor it affected cytotoxicity of free DOX, it could increase the toxicity of DOX encapsulated in both types of NPs (**Figure 2f**) and in particular of the DOX-loaded EMNVs showing a significant decrease of cell viability in comparison with free DOX. We justify this phenomenon with the ability of HCQ to decrease endosomal sequestration of the carriers and their payloads. Finally, we investigated if the observed toxicity could be the result of DOX-induced apoptosis by investigating the activation of Caspase-3 [26] using a reporter assay. Adding DOX or DOX-loaded NPs, we observed a consistent activation of this apoptotic mediator in all the samples delivering the chemotherapeutic, highlighting a similar working mechanism of EVs and EMNVs (**Figure 2g, h**).

## 4. Conclusions

In this work, we directly compared the performances of EVs and EMNVs in delivering DOX. Despite the remarkable differences in their manufacturing, the particles showed comparable physical, biological and cytotoxic features. Our study revealed also a significant increase in cytotoxicity of either type of DOX-loaded NPs when combined with an FDA-approved drug HCQ. This is the first indication that a lysosome destabilizer can improve the performance of biological NPs.

More investigation is necessary to evaluate if these benefits persist in different experimental scenarios (i.e., encapsulating other therapeutics, in vivo biodistribution, targeting, efficacy and side effects), but it is important to highlight that EMNVs can serve as delivery model in many studies, providing a cost-effective and high-reproducible tool to investigate biomimetic particle properties. At the same time, the use of endolysosomal destabi-

 doi:10.20944/preprints202212.0060.v1

lizing compound can remarkably improve the performance of biological NPs as previously shown with synthetic carriers[19], [33], and for this reason more insights about this pharmacologic combinations should be gathered.

**Author Contributions:** Conceptualization, D.K., S.B., A.P.; methodology, S.B., N.P., A.K., E.B., A.F., O.S., L.F.; software, S.B., A.K., E.B., O.S., L.F.; validation, S.B., N.P., A.K., A.F., O.S.; formal analysis, G.M., M.Z., I.G., S.M., A.Z., V.C, A.P.; investigation, S.B., A.K., E.K., O.S., D.K.; resources, G.M., M.Z., I.G., S.M., A.Z., V.C., D.K.; data curation, S.B., A.K., D.K.; writing—original draft preparation, A.P., D.K., S.B.; writing—review and editing, A.P., A.Z., D.K., S.B.; visualization, A.K., S.B.; supervision, D.K.; project administration, A.Z., V.C., A.P., D.K.; funding acquisition, A.Z. All authors have read and agreed to the published version of the manuscript.

**Funding:** This research was funded by RSF, grant number 21-75-30020.

**Data Availability Statement:** all data available is presented in the body of the manuscript.

**Conflicts of Interest:** The authors declare no conflict of interest.

## References

[1] X. Luan, K. Sansanaphongpricha, I. Myers, H. Chen, H. Yuan, and D. Sun, "Engineering exosomes as refined biological nanoplatforms for drug delivery.," *Acta Pharmacol. Sin.*, vol. 38, no. 6, pp. 754–763, Jun. 2017, doi: 10.1038/aps.2017.12.

[2] J. C. Akers, D. Gonda, R. Kim, B. S. Carter, and C. C. Chen, "Biogenesis of extracellular vesicles (EV): exosomes, microvesicles, retrovirus-like vesicles, and apoptotic bodies," *J. Neurooncol.*, vol. 113, no. 1, pp. 1–11, 2013.

[3] D. Ha, N. Yang, and V. Nadithe, "Exosomes as therapeutic drug carriers and delivery vehicles across biological membranes: current perspectives and future challenges," *Acta Pharm. Sin. B*, vol. 6, no. 4, pp. 287–296, 2016.

[4] S. Kamerkar *et al.*, "Exosomes facilitate therapeutic targeting of oncogenic KRAS in pancreatic cancer.," *Nature*, vol. 546, no. 7659, pp. 498–503, Jun. 2017, doi: 10.1038/nature22341.

[5] Y. Liang, L. Duan, J. Lu, and J. Xia, "Engineering exosomes for targeted drug delivery," *Theranostics*, vol. 11, no. 7, p. 3183, 2021.

[6] P. Saha *et al.*, "Circulating exosomes derived from transplanted progenitor cells aid the functional recovery of ischemic myocardium," *Sci. Transl. Med.*, vol. 11, no. 493, p. eaau1168, 2019.

[7] L. Mao *et al.*, "Heart-targeting exosomes from human cardiosphere-derived cells improve the therapeutic effect on cardiac hypertrophy," *J. Nanobiotechnology*, vol. 20, no. 1, pp. 1–14, 2022.

[8] W. Zhou *et al.*, "Pancreatic cancer-targeting exosomes for enhancing immunotherapy and reprogramming tumor microenvironment," *Biomaterials*, vol. 268, p. 120546, 2021.

[9] S. Li, Z. Lin, X. Jiang, and X. Yu, "Exosomal cargo-loading and synthetic exosome-mimics as potential therapeutic tools," *Acta Pharmacol. Sin.*, vol. 39, no. 4, pp. 542–551, 2018.

[10] X. Jia, J. Tang, C. Yao, and D. Yang, "Recent progress of extracellular vesicle engineering," *ACS Biomater. Sci. Eng.*, vol. 7, no. 9, pp. 4430–4438, 2021.

[11] T. R. Lunavat *et al.*, "RNAi delivery by exosome-mimetic nanovesicles–Implications for targeting c-Myc in cancer," *Biomaterials*, vol. 102, pp. 231–238, 2016.

[12] L. I. Sun *et al.*, "Safety evaluation of exosomes derived from human umbilical cord mesenchymal stromal cell," *Cytotherapy*, vol. 18, no. 3, pp. 413–422, 2016.

[13] I. Kimiz-Gebologlu and S. S. Oncel, "Exosomes: Large-scale production, isolation, drug loading efficiency, and biodistribution and uptake," *J. Control. Release*, vol. 347, pp. 533–543, 2022.

[14] W. Jo *et al.*, "Large-scale generation of cell-derived nanovesicles," *Nanoscale*, vol. 6, no. 20, pp. 12056–12064, 2014.

[15] A. A. Al-Dossary *et al.*, "Engineered EV-Mimetic Nanoparticles as Therapeutic Delivery Vehicles for High-Grade Serous Ovarian Cancer," *Cancers (Basel).*, vol. 13, no. 12, p. 3075, 2021.

[16] D. Kostyushev *et al.*, "Gene Editing by Extracellular Vesicles," *Int. J. Mol. Sci.*, vol. 21, no. 19, p. 7362, 2020.

[17] S. E. L. Andaloussi, S. Lakhal, I. Mäger, and M. J. A. Wood, "Exosomes for targeted siRNA delivery across biological barriers," *Adv. Drug Deliv. Rev.*, vol. 65, no. 3, pp. 391–397, 2013.

[18] S. A. Meo, D. C. Klonoff, and J. Akram, "Efficacy of chloroquine and hydroxychloroquine in the treatment of COVID-19.," *Eur Rev Med Pharmacol Sci*, pp. 4539–4547, 2020.

[19] A.-L. Tian *et al.*, "Lysosomotropic agents including azithromycin, chloroquine and hydroxychloroquine activate the integrated stress response," *Cell Death Dis.*, vol. 12, no. 1, pp. 1–13, 2021.

[20] J. Wolfram *et al.*, "A chloroquine-induced macrophage-preconditioning strategy for improved nanodelivery," *Sci. Rep.*, vol. 7, no. 1, pp. 1–13, 2017.

[21] H. Maes, A. Kuchnio, P. Carmeliet, and P. Agostinis, "Chloroquine anticancer activity is mediated by autophagy-independent effects on the tumor vasculature," *Mol. Cell. Oncol.*, vol. 3, no. 1, p. e970097, 2016.

[22] G. Gao *et al.*, "Intracellular Nanoparticle Formation and Hydroxychloroquine Release for Autophagy-Inhibited Mild-Temperature Photothermal Therapy for Tumors," *Adv. Funct. Mater.*, vol. 31, no. 34, p. 2102832, 2021.

 doi:10.20944/preprints202212.0060.v1

[23] Y. Li, M. H. Cho, S. S. Lee, D.-E. Lee, H. Cheong, and Y. Choi, "Hydroxychloroquine-loaded hollow mesoporous silica nanoparticles for enhanced autophagy inhibition and radiation therapy," *J. Control. Release*, vol. 325, pp. 100–110, 2020.
[24] A. A. Stepanenko and V. V Dmitrenko, "HEK293 in cell biology and cancer research: phenotype, karyotype, tumorigenicity, and stress-induced genome-phenotype evolution," *Gene*, vol. 569, no. 2, pp. 182–190, 2015.
[25] S. Rivankar, "An overview of doxorubicin formulations in cancer therapy," *J. Cancer Res. Ther.*, vol. 10, no. 4, p. 853, 2014.
[26] T.-L. To *et al.*, "Rational Design of a GFP-Based Fluorogenic Caspase Reporter for Imaging Apoptosis In Vivo.," *Cell Chem. Biol.*, vol. 23, no. 7, pp. 875–882, Jul. 2016, doi: 10.1016/j.chembiol.2016.06.007.
[27] R. Kornilov *et al.*, "Efficient ultrafiltration-based protocol to deplete extracellular vesicles from fetal bovine serum," *J. Extracell. vesicles*, vol. 7, no. 1, p. 1422674, 2018.
[28] N. Heath *et al.*, "Rapid isolation and enrichment of extracellular vesicle preparations using anion exchange chromatography," *Sci. Rep.*, vol. 8, no. 1, pp. 1–12, 2018.
[29] V. S. Chernyshev *et al.*, "Size and shape characterization of hydrated and desiccated exosomes," *Anal. Bioanal. Chem.*, vol. 407, no. 12, pp. 3285–3301, 2015.
[30] H.-K. Woo, Y. K. Cho, C. Y. Lee, H. Lee, C. M. Castro, and H. Lee, "Characterization and modulation of surface charges to enhance extracellular vesicle isolation in plasma," *Theranostics*, vol. 12, no. 5, p. 1988, 2022.
[31] M. C. Deregibus *et al.*, "Charge-based precipitation of extracellular vesicles," *Int. J. Mol. Med.*, vol. 38, no. 5, pp. 1359–1366, 2016.
[32] C. Théry *et al.*, "Minimal information for studies of extracellular vesicles 2018 (MISEV2018): a position statement of the International Society for Extracellular Vesicles and update of the MISEV2014 guidelines," *J. Extracell. vesicles*, vol. 7, no. 1, p. 1535750, 2018.
[33] F. Perche *et al.*, "Hydroxychloroquine-conjugated gold nanoparticles for improved siRNA activity," *Biomaterials*, vol. 90, pp. 62–71, 2016.
[34] G. Marcelo, E. Kaplan, M. P. Tarazona, and F. Mendicuti, "Interaction of gold nanoparticles with Doxorubicin mediated by supramolecular chemistry," *Colloids Surfaces B Biointerfaces*, vol. 128, pp. 237–244, 2015.